A radio continuum and HI study of IC63, IC59, and IRAS 00556+6048: Nebulae in the vicinity of gamma Cas

Blouin, D.; McCutcheon, W.H.; Dewdney, P.E.; Roger, R.S.; Purton, C.R.; Kester, D.J.M.; Bontekoe, Tj.R.

DOI
10.1093/mnras/287.2.455

Publication date
1997

Published in
Monthly Notices of the Royal Astronomical Society

Mon. Not. R. Astron. Soc. **287,** 455–471 (1997)

A radio continuum and H I study of IC 63, IC 59, and IRAS 00556 + 6048: nebulae in the vicinity of γ Cas

D. Blouin,[1] W. H. McCutcheon,[2] P. E. Dewdney,[3] R. S. Roger,[3] C. R. Purton,[3] D. Kester[4] and Tj. R. Bontekoe[5]

[1] *# 3 St-Amable, St-Guillaume, PQ J0C 1L0, Canada*
[2] *Department of Physics and Astronomy, University of British Columbia, Vancouver, BC V6T 1Z1, Canada*
[3] *Dominion Radio Astrophysical Observatory, Herzberg Institute of Astrophysics, National Research Council, PO Box 248, Penticton, BC V2A 6K3, Canada*
[4] *Space Research, PO Box 800, NL-9700 AV Groningen, the Netherlands*
[5] *Bontekoe Data Consultancy, Herengracht 47, 2312 LC Leiden, the Netherlands*

Accepted 1997 January 10. Received 1996 December 31; in original from 1996 August 15

ABSTRACT

Sh 185, which is associated with the B0–B0.5IV star γ Cas and contains the two nebulae IC 63 and IC 59, has been observed with the DRAO synthesis telescope in continuum emission at 408 and 1420 MHz, and in H I line emission. Continuum emission is clearly detected for IC 63 and weakly detected for IC 59. The emission from both nebulae is thermal, with the masses of ionized gas being 0.08 and 0.07 $M_\odot$, respectively. The masses of H I detected are 0.15 $M_\odot$ for IC 63, and 0.64 $M_\odot$ for IC 59. Infrared emission was detected in the *IRAS* survey from both IC 63 and IC 59, and also from a point source, IRAS 00556 + 6048, located between the two clouds. The infrared and radio luminosities of IC 63 and IC 59 are consistent with the heating and ionization being produced by γ Cas. However, the time required to produce the observed H I through photodissociation is less than any reasonable age for γ Cas by orders of magnitude. This suggests that the nebulae are density-bounded and the production of H I through photodissociation by radiation from γ Cas has mostly ceased. The exception occurs in a small region of molecular gas in IC 63, where extended red emission and molecular hydrogen fluorescent emission are still observed. H I is also detected near IRAS 00556 + 6048. This H I appears to be associated with the infrared source, and with a velocity of -34 km s^{-1} suggests that the infrared source is not associated with Sh 185. The exciting star for IRAS 00556 + 6048 may be another example of a dissociating star.

Key words: infrared: ISM: continuum – radio continuum: ISM – radio lines: ISM.

1 INTRODUCTION

Sh 185 is a region of nebulosity, consisting principally of two comet-shaped clouds, IC 63 and IC 59. These clouds, located 20 arcmin to the north-east from the nearby ($\sim$230 pc) B0–B0.5IV star, γ Cas (Figs 1a and b, opposite p. 456), exhibit marked differences between their colours and morphological structures (Osterbrock 1957; van den Bergh 1966). IC 63 is characterized by the presence of strong filaments (Figs 2 and 3), whose optical emission appears to be predominantly red. The emission from IC 59 is bluer and no filamentary structure is observed.

Witt et al. (1989) observed strong molecular hydrogen fluorescent emission and extended red emission (ERE) in IC 63 but not in IC 59, although both clouds were found to have similar emission spectra in the 600–700 nm region, indicating closely matched excitation conditions. The complex UV fluorescence spectrum observed in IC 63, predicted to occur in diffuse interstellar clouds and reflection nebulae by Duley & Williams (1980), is a striking signature of a photodissociation region. The excitation of hydrogen molecules by absorption of UV photons, and the subsequent relaxation, is the primary process for the dissociation of H_2 (Stecher & Williams 1967). The ERE is attributed to lumi-

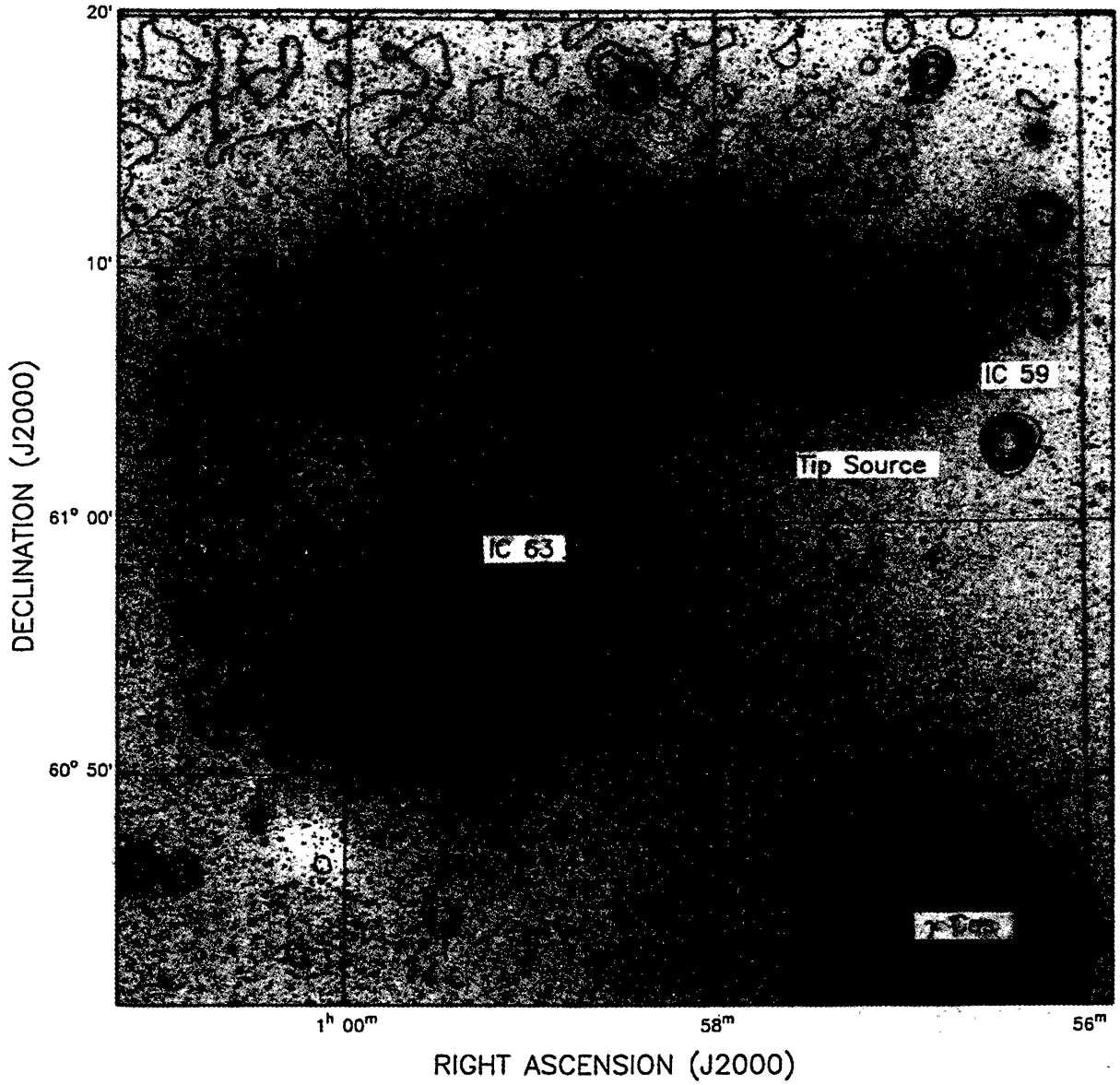

Figure 2. *E*-band print of the Sh 185 region reproduced from Poeckert & van den Berg (1981) overlaid with contours of 21-cm continuum emission observed at DRAO. The contour levels are 1.3, 1.5, 1.7, 2.0, 2.5, and 3.0 K.

nescence by hydrogenated amorphous carbon grains (Witt & Schild 1988; Jones, Duley & Williams 1990). The presence of UV fluorescence and ERE strongly indicate the formation of a zone of H I, formed through dissociation of H_2, around IC 63.

The observations of resonant fluorescence of molecular hydrogen in IC 63 were made by Witt et al. in the brightest tip of the nebula facing γ Cas. They estimated that the intensity of the UV field at 100 nm, that is incident upon the surface, is $\sim 4.6 \times 10^{-4}$ erg cm^{-2} s^{-1} Å^{-1}, or $\sim 2.3 \times 10^{-5}$ photon cm^{-2} s^{-1} Hz^{-1} (see Sternberg 1989). This flux is 671 times the value of the average interstellar field (Sternberg 1989). For some clouds, which are illuminated only by the general interstellar radiation field, H I has been detected as limb-brightening at the edges (van der Werf et al. 1989; Wannier et al. 1991). Thus an H I zone associated with IC 63 should be detectable in emission. Given the spectral type of γ Cas, bremsstrahlung emission from ionized hydrogen and infrared emission from dust should be detectable as well.

IC 63 is an ideal example of a photodissociation region which can be studied at high linear resolution (0.06 pc arcmin^{-1}) and which has a well-known source of UV illumination. IC 59, with its contrasting properties, provides an interesting comparison study. The relatively simple geometry of Sh 185, and the absence of absorbing material between Sh 185 and γ Cas, provide an opportunity to compare accurately the emission from these components with the exciting star properties. Comparison of results from H I observations with the hydrogen dissociation model of Roger & Dewdney (1992) will help us to understand the time development of any H I zones around IC 63 and IC 59.

Opposite p. 456, MNRAS, **287**

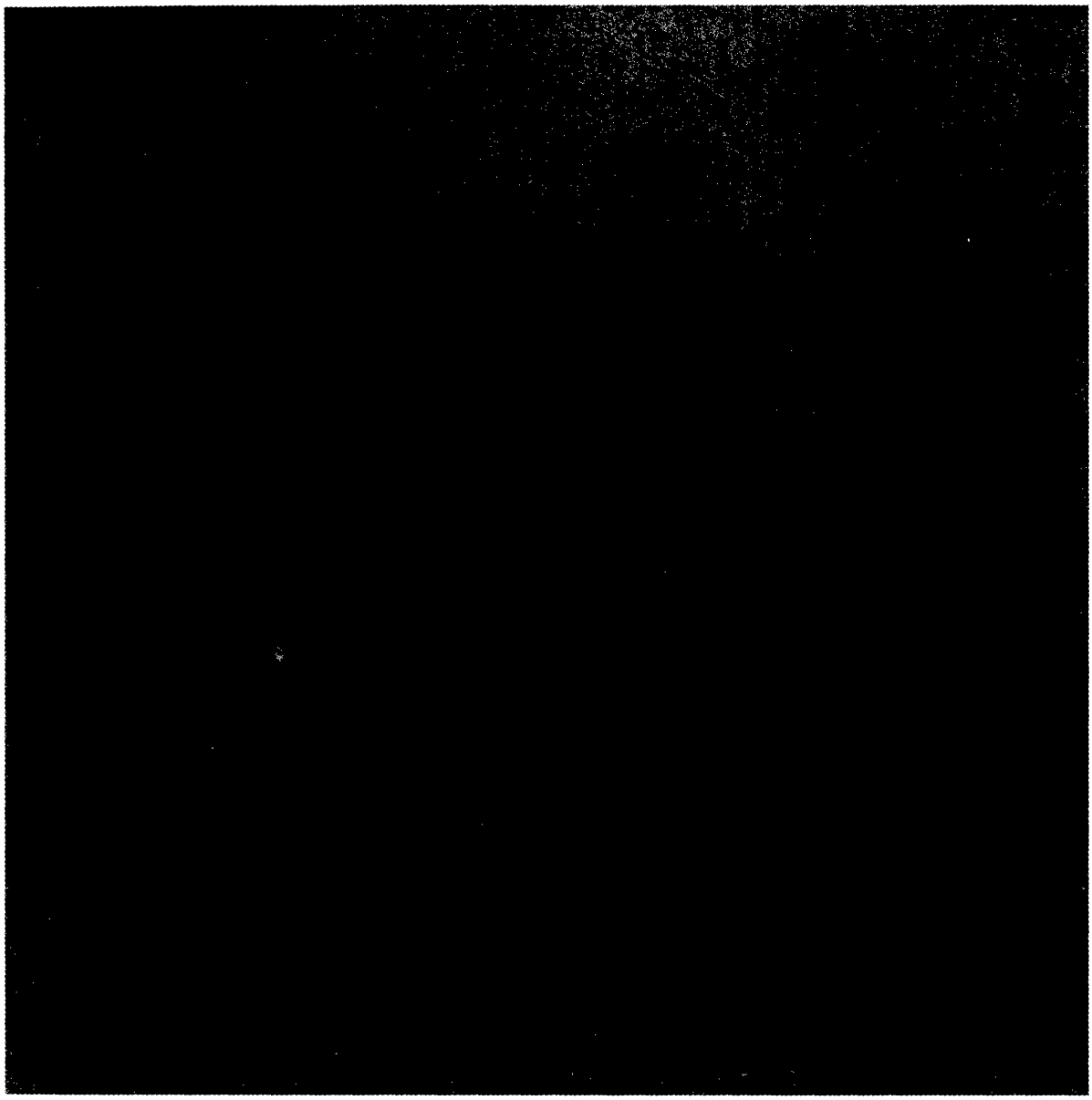

Figure 1. Sh 185 and the star γ Cas reproduced from the Palomar Observatory Survey (a) red print and (b) blue print. North is toward the top and east to the left. γ Cas is the brightest star near the centre and is the exciting star for Sh 185. IC 63, to the north-east of γ Cas, appears bright on both prints. IC 59, to the north of γ Cas, is bright only on the blue print. The scale is 7 arcmin cm^{-1}.

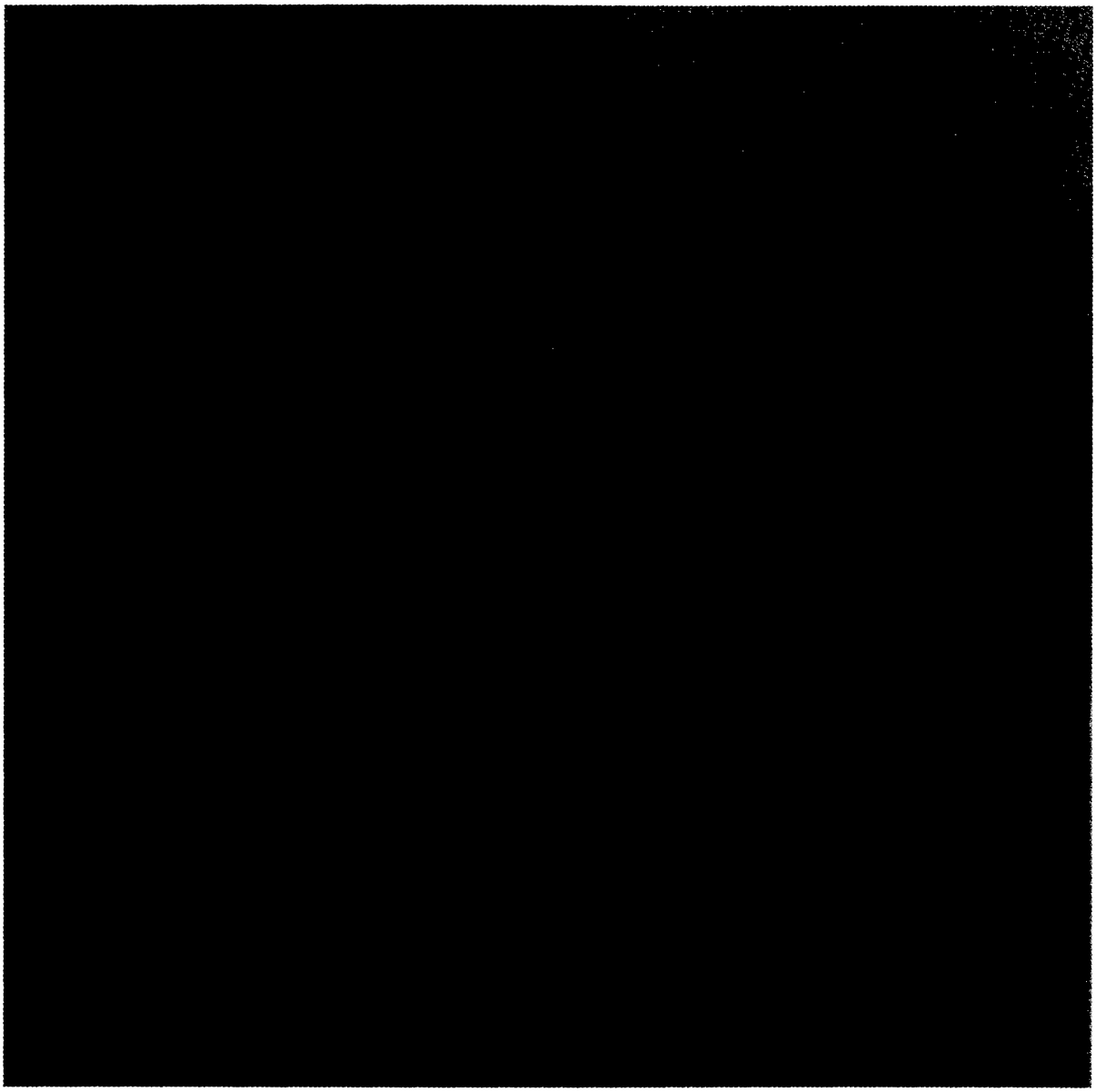

Figure 1 – *continued*

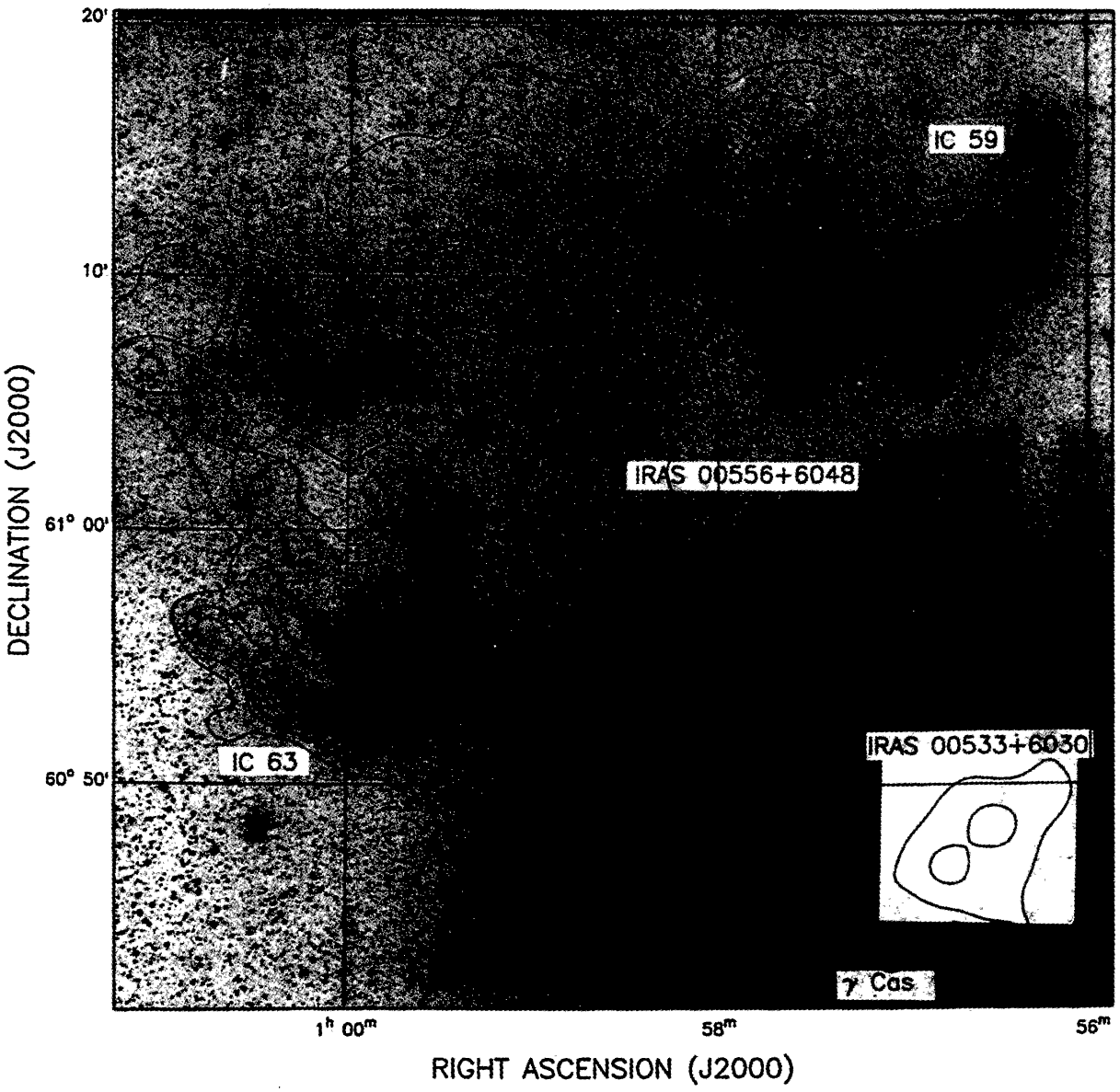

Figure 3. *J*-band print of the Sh 185 region reproduced from Poeckert & van den Berg (1981) overlaid with contours of 60-μm emission. The contour levels are 9, 13, 17, 30, 40, 50, and 60 MJy sr^{-1}. The 60-μm emission map is processed at high resolution (1 arcmin) from the *IRAS* survey data in Groningen (Assendorp et al. 1995; see Section 3.2).

2 PROPERTIES OF γ CAS

γ Cas has the characteristics of an emission-line star and has been classified both as a B0IVnpe (Garrison & Beattie 1996) and a B0.5IVe (Lesh 1968; Slettebak 1982).

The star exhibits variability, with the apparent magnitude varying between 1.5 and 2.7 since 1930 (Cowley, Roger & Hutchings 1976). This represents a change in luminosity by a factor of 3. At present the luminosity is increasing slowly. This variability may be the result of an optically thick disc expanding to an optically thin spherical shape (Kogure 1990).

There is considerable range in the published values of the distance to γ Cas, from 224 pc (Garrison & Beattie 1996) to 442 pc (Fabregat & Reglero 1990). We have adopted the distance of 230 ± 70 pc from Vakili, Granes & Bonneau (1984). The distance is strongly dependent on spectral type, and the adopted distance given above is for the spectral type B0.5IV. For a B0IV star with the same apparent magnitude, the distance would be increased by a factor of 1.13.

Blouin (1994) obtained the non-ionizing luminosity of the star, $L = (1.4 \pm 0.5) \times 10^{31}$ W, from the continuous energy distribution of Waters et al. (1991). Using a Kurucz model (Kurucz 1979) fitted to the distribution, the ionizing luminosity can be inferred. The ratio of the ionizing to non-ionizing luminosity is 0.0032, so that the luminosity quoted above is essentially the same as the total luminosity of the star. Using this luminosity, the number of ionizing photons, $N_{L*} = (5.5 \pm 1.5) \times 10^{46}\ s^{-1}$, is obtained from the tables of Panagia (1973).

An upper limit for the age of γ Cas can be inferred as follows. For a main-sequence star with an absolute magnitude of ~ -4, the mass is $\sim 16\ M_{\odot}$, and the corresponding available energy is 2.0×10^{45} J (Böhm-Vitense 1992). With

the above luminosity, the longest main-sequence evolution time $\sim 4.5 \times 10^6$ yr.

3 OBSERVATIONS

3.1 DRAO observations

IC 63, IC 59 and associated nebulae were mapped at 408 and 1420 MHz with the seven-element, wide-field Synthesis Telescope at the Dominion Radio Astrophysical Observatory (DRAO) in 1992 October. This was one of the first surveys undertaken after the array upgrade to seven antennae. The field sizes (to 20 per cent response) and synthesized beams (east–west by north–south) are respectively 8.1° and 3.5×4.0 arcmin^2 at 408 MHz, and 2.6° and 1.0×1.14 arcmin^2 at 1420 MHz.

The observations consisted of measurements of 12 h duration at all interferometer spacings from 13 to 600 m (4.3-m interval), giving complete UV coverage in that range. Maps were made by Fourier-transforming calibrated, gridded visibilities, and the continuum maps were CLEANed. Both H I and continuum data are corrected for the attenuation of the primary beams of the 9-m paraboloids of the array.

Extended structure in both H I-line and 1420-MHz continuum, corresponding to interferometer spacings less than 13m, was extracted from single antenna observations. For H I emission, the region was mapped with the DRAO 26-m paraboloid and calibrated with the standard region S7 (Williams 1973). For the 1420-MHz continuum emission, data were taken from the Effelsberg 1.4-GHz survey of Kallas & Reich (1980).

The continuum bandwidths used were 4 MHz at 408 MHz, and 30 MHz at 1420 MHz. The line emission is observed with a 128-channel spectrometer with bandwidth 0.5 MHz, giving a channel width of 0.66 km s^{-1}. In continuum, the measured rms noise levels at the centre of the fields are 8.2 mJy beam^{-1} at 408 MHz, and 0.4 mJy beam^{-1} at 1420 MHz. For each spectral channel, the rms noise at the field centre is 4.2 K on blank sky, and perhaps 2 to 3 K higher for regions of strong H I emission.

3.2 Other related observations and surveys

A $2° \times 2°$ region centred on γ Cas was mapped in ^{12}CO, $J=1$–0, with the Five Colleges Radio Astronomy Observatory (FCRAO) 15-m telescope and QUARRY receiver. A coincident $1° \times 1°$ region was mapped in ^{13}CO. Both maps were made at single-beam spacing and with channel widths of 250 kHz. Channel rms noises are about 0.44 K in ^{12}CO, and about 0.22 K in ^{13}CO.

Six selected positions in IC 63, IC 59 and the surrounding region were observed in the $J=2$–1 CO line using the James Clerk Maxwell Telescope (JCMT). Integration times of 3 and 5 min on source yielded rms noises of 260 and 200 mK, respectively.

Other radio-continuum emission information was obtained at 6 cm from the National Radio Astronomy Observatory (NRAO) survey (Condon, Broderick & Seielstad 1989), at 11 cm from the Bonn survey (Reich et al. 1990), and at 21 cm from both Bonn and NRAO surveys (Kallas & Reich 1980; Condon & Broderick 1986).

Infrared emission data were obtained from the *IRAS* All-Sky Survey, and also from a 60-μm high-resolution map which was made from the *IRAS* survey data contained on the *IRAS* server system in Groningen (Assendorp et al. 1995). For the Groningen 60-μm data, a zodiacal model was subtracted from the data and residual background emission was removed. The high-resolution map was made using the Pyramid Maximum Entropy method (Bontekoe, Koper & Kester 1994). The resolution in this map is somewhat dependent on the local signal-to-noise ratios, but is estimated to be about 1 arcmin on pixels of 15 arcsec size. The photometric quality in this map is expected to be somewhat less than in the standard *IRAS* products.

Optical data were obtained from the Palomar Observatory Sky Survey (POSS) prints, and also from prints kindly supplied by Dr S. van den Bergh, from the data of Poeckert & van den Bergh (1981).

4 RESULTS

4.1 Far-infrared emission

The 60-μm observations of Sh 185 are shown in Figs 3, 4 (upper), and 5. Fig. 3 shows the *J*-band print reproduced from Poeckert & van den Bergh (1981), overlaid with contours of the *IRAS* 60-μm emission processed at high (1 arcmin) resolution from the Groningen *IRAS* data system. Infrared emission from IC 63 and IC 59 is clearly detected and matches the optical emission closely. Emission is also detected in the other *IRAS* bands (12, 25 and 100 μm). However, high-resolution maps are not yet available for these bands.

Integrated far-infrared flux densities and dust temperatures for IC 63 and IC 59 are listed in Table 1. Emission from the entire clouds (including tips and wings) was summed and background subtracted. The resulting fluxes were then colour-corrected (Beichman et al. 1985, IRAS Explanatory Supplement) assuming a thermal spectral distribution with emissivity $Q_U = \varepsilon \nu^\beta$ with $\beta = 1$. The dust temperature T_D was computed from the ratio of the total power received in the 60- and 100-μm bands.

4.2 Radio continuum emission

The 21-cm continuum emission of Sh 185 observed with the DRAO telescope is displayed in Figs 2 and 6. These images include the short spacing data (see Section 3.1). Fig. 2 shows contours of the 21-cm continuum emission overlaid with the *E*-band print of Poeckert & van den Bergh (1981). Continuum emission from IC 63 is clearly detected and matches the optical emission closely. Continuum emission from IC 59 is weaker and it is difficult to determine the edges of the cloud precisely. A point source (hereafter called the Tip Source) is observed right at the tip of IC 59, between γ Cas and the cloud.

Table 2 lists radio continuum fluxes for IC 63, IC 59 and the Tip Source. These flux densities were background subtracted and again include all emission from the wings and tips of the clouds. The flux density for IC 59 was integrated inside a boundary defined by the optical emission of the cloud, since radio continuum emission from IC 59 is not easily separated from the background.

Fig. 7 shows spectra for these sources. Flux densities at 6, 11 and 74 cm were obtained from the surveys of Condon et

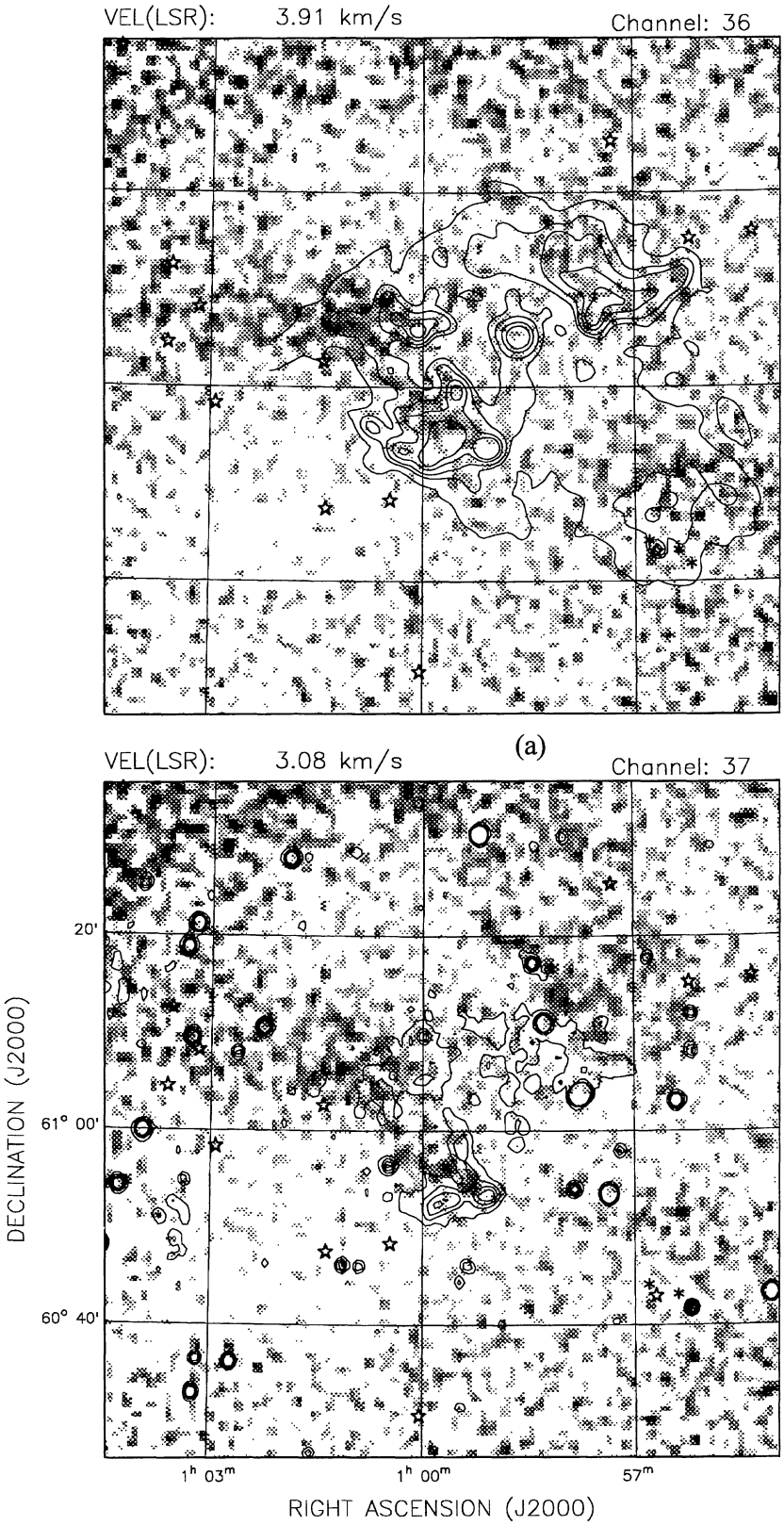

Figure 4. H I emission associated with IC 63 and IC 59 represented by the grey-scale, which varies continuously from 2 K (white) to 20 K (black). The bottom images of (a) to (d) show overlaid contours at 1.4 and 1.7 K of the DRAO 21-cm continuum emission, while the upper images of (a) to (d) show overlaid contours, starting at 7 MJy sr^{-1} in steps of 5 MJy sr^{-1}, from the *IRAS* 60-μm high-resolution data from the Groningen *IRAS* data system. The five point stars on all images indicate positions of the brightest stars in the field. H I emission from IC 63 and IC 59, detected over the velocity range 3.08 to -1.04 km s^{-1} inclusive (channels 37 to 42), is shown in (a) to (d).

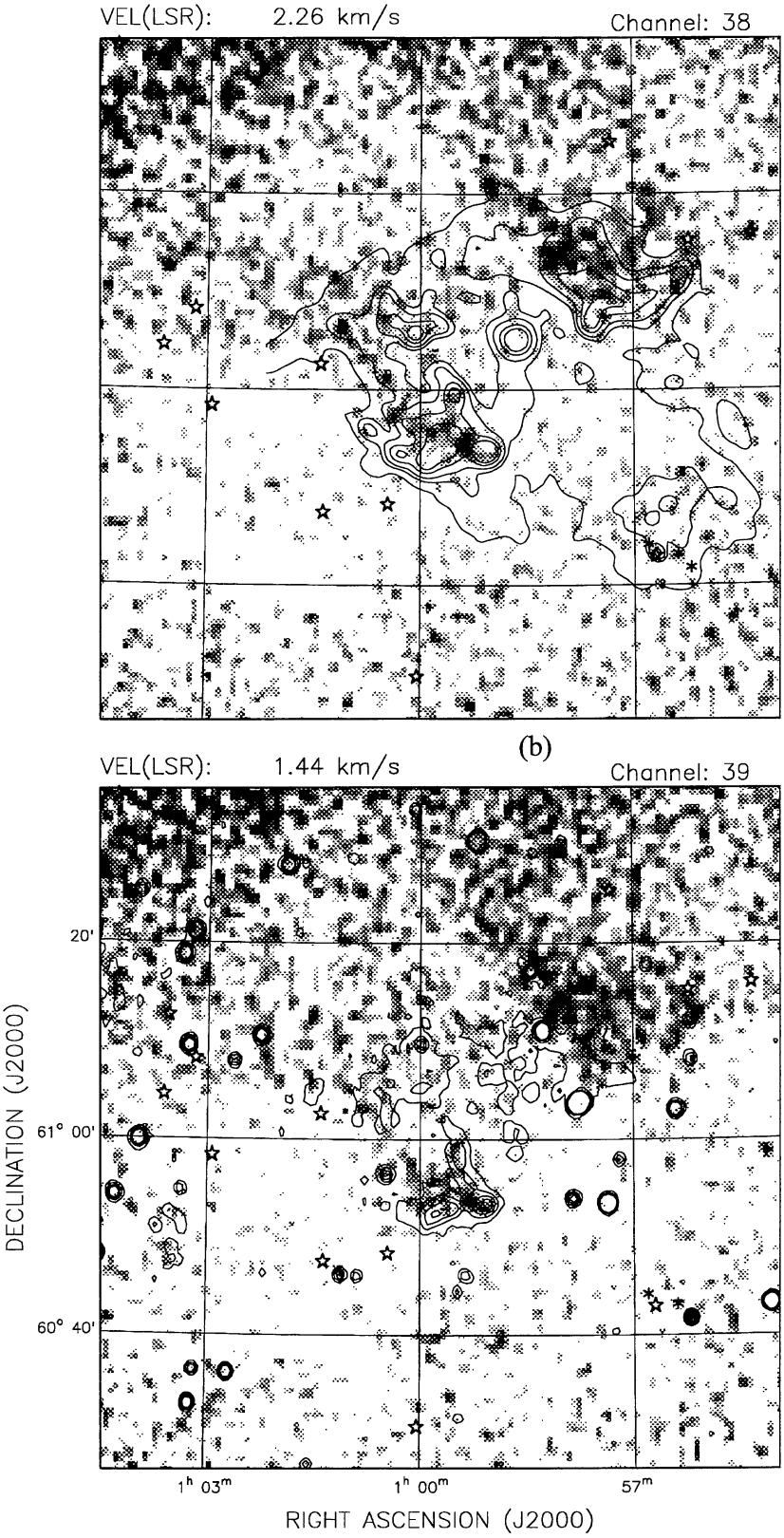

Figure 4 – *continued*

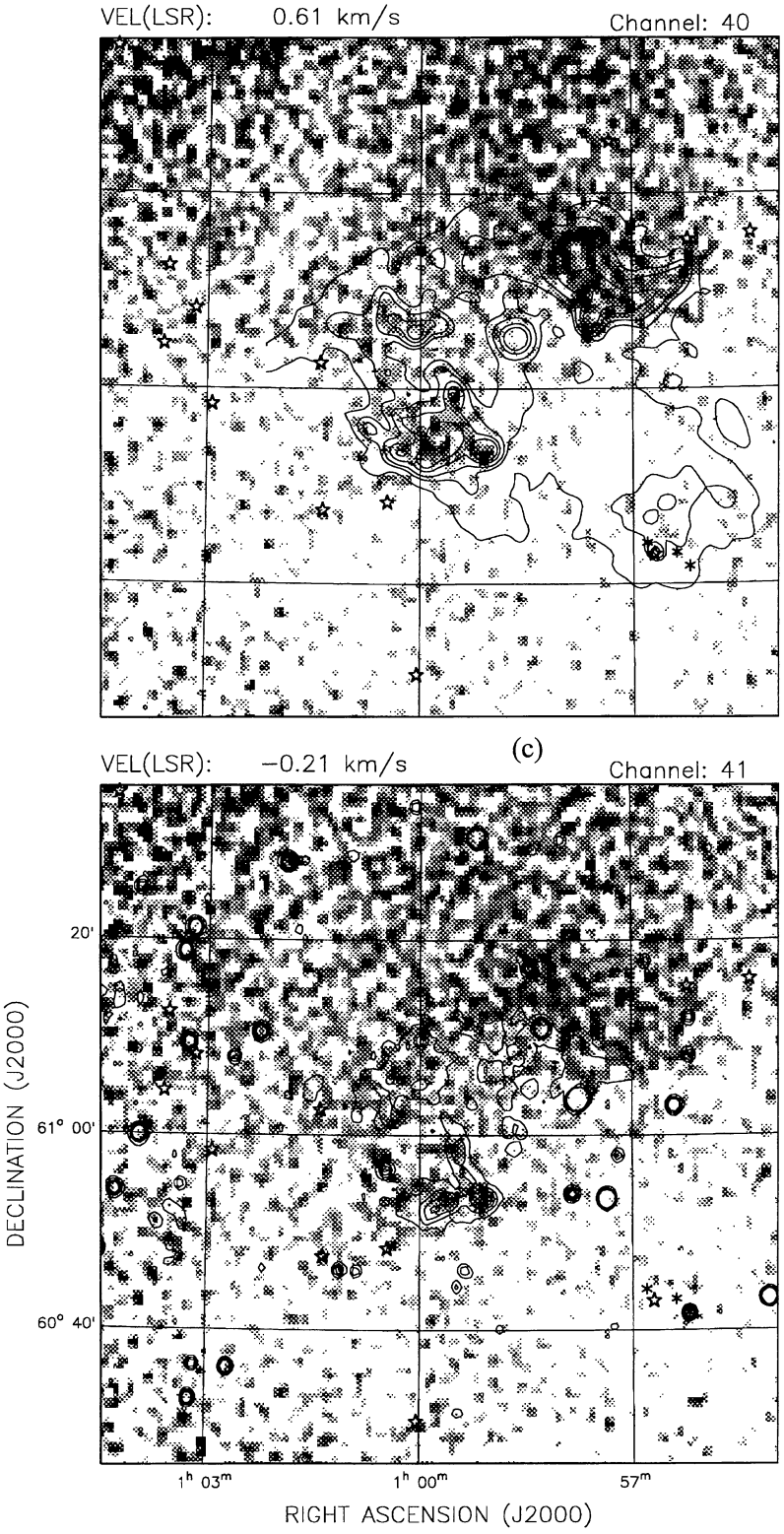

Figure 4 – *continued*

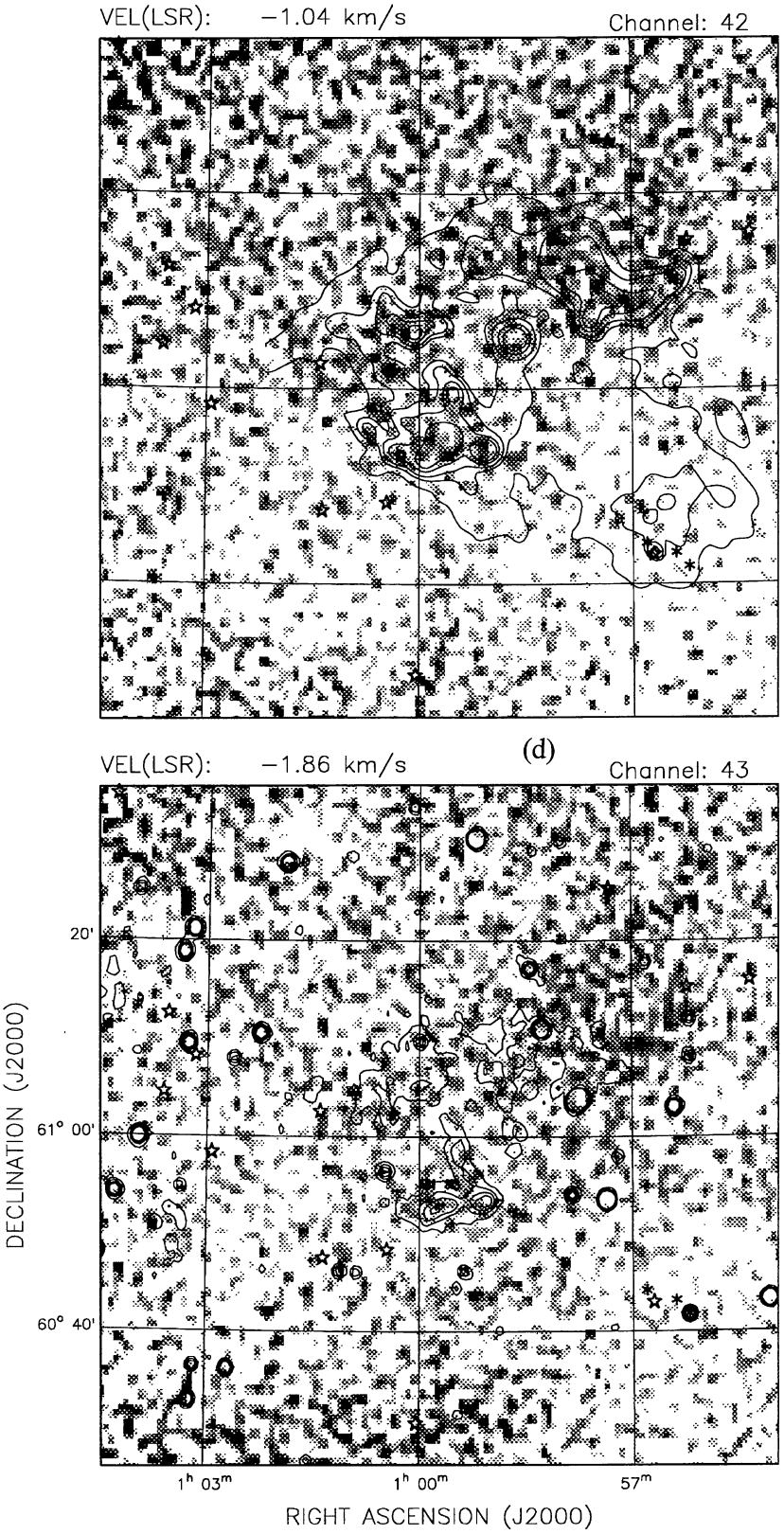

Figure 4 – *continued*

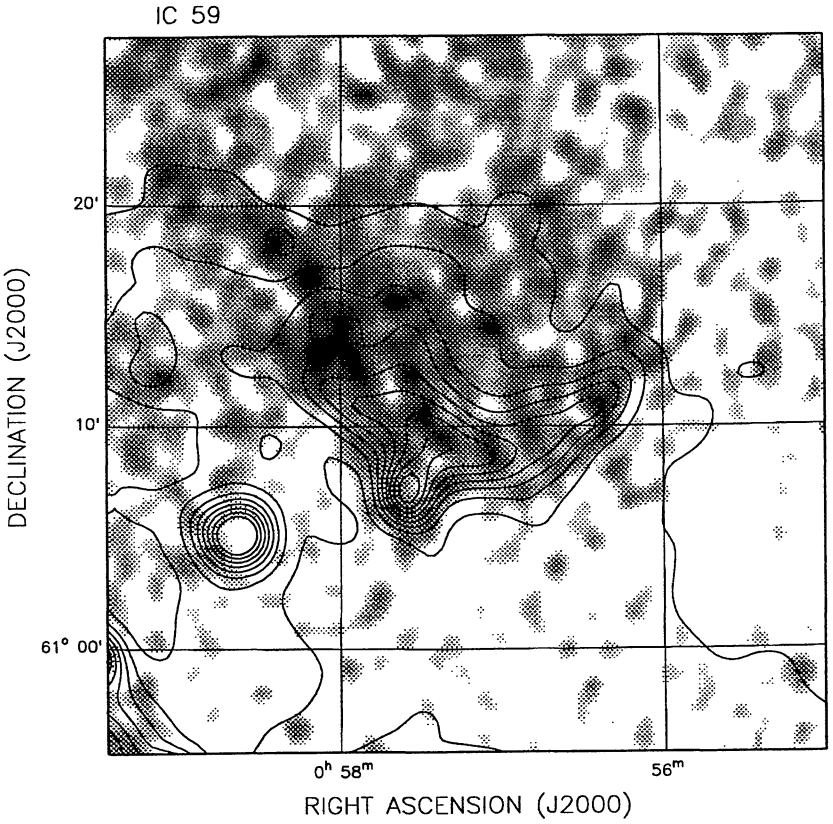

Figure 5. H I column density map for IC 59 [grey-scale: 9.0×10^{20} atom cm^{-2} (black areas), 7.1×10^{20} atom cm^{-2} (white areas), with a large background component of column density]. The contours represent the *IRAS* 60-μm high-resolution map starting at 5 MJy sr^{-1} in steps of 5 MJy sr^{-1}.

Table 1. Integrated flux densities, S_λ (Jy), at four wavelengths, and the derived dust temperatures (K).

Source	$S_{12\mu m}$	$S_{25\mu m}$	$S_{60\mu m}$	$S_{100\mu m}$	T_D[3]
IC 63[1]	19.0±0.4	23±1	230±10	350±10	41
IC 59[1]	20.3±0.5	18±1	170±10	390±10	34
IRAS 00556+6048[2]	4.7±0.4	29±2	110±20	140±20	45

Notes:
[1]Flux densities for IC 59 and IC 63 are integrated from the *IRAS* Sky Survey Atlas. uncertainties due to noise and background confusion are estimated by integrating over slightly different source boundaries.
[2]Flux densities for IRAS 00556 + 6048 are taken from the *IRAS* Point Source Catalogue.
[3]Colour temperatures calculated from the 60- and 100-μm flux densities.

al. (1989), Reich et al. (1990), and from our observations at 408 MHz with the DRAO synthesis telescope. It is clear that emission from IC 63 and IC 59 is thermal while that of the Tip Source is non-thermal, so it is unlikely to be associated with IC 59.

4.3 Line emission

4.3.1 H I line emission

H I emission from Sh 185 is detected over a velocity range of 7 km s^{-1} centred approximately on $V_{LSR} = 1.0$ km s^{-1}. The cometary shape of the clouds clearly identified on the H I emission (Fig. 4) insures the association of this weak component with the other IR and radio counterparts of the clouds. Moreover, the velocity of the H I emission is close to the velocity of -3.46 km s^{-1} (Cowley et al. 1976) for γ Cas. Although they do not state whether this velocity is given with respect to the local standard of rest (LSR) or to the Sun, the difference in velocity between the two references is only a few km s^{-1}. Figs 8 and 5 show averaged H I maps for IC 63 and IC 59. The emission is relatively weak but is well confined, especially for IC 63. As expected, the continuum

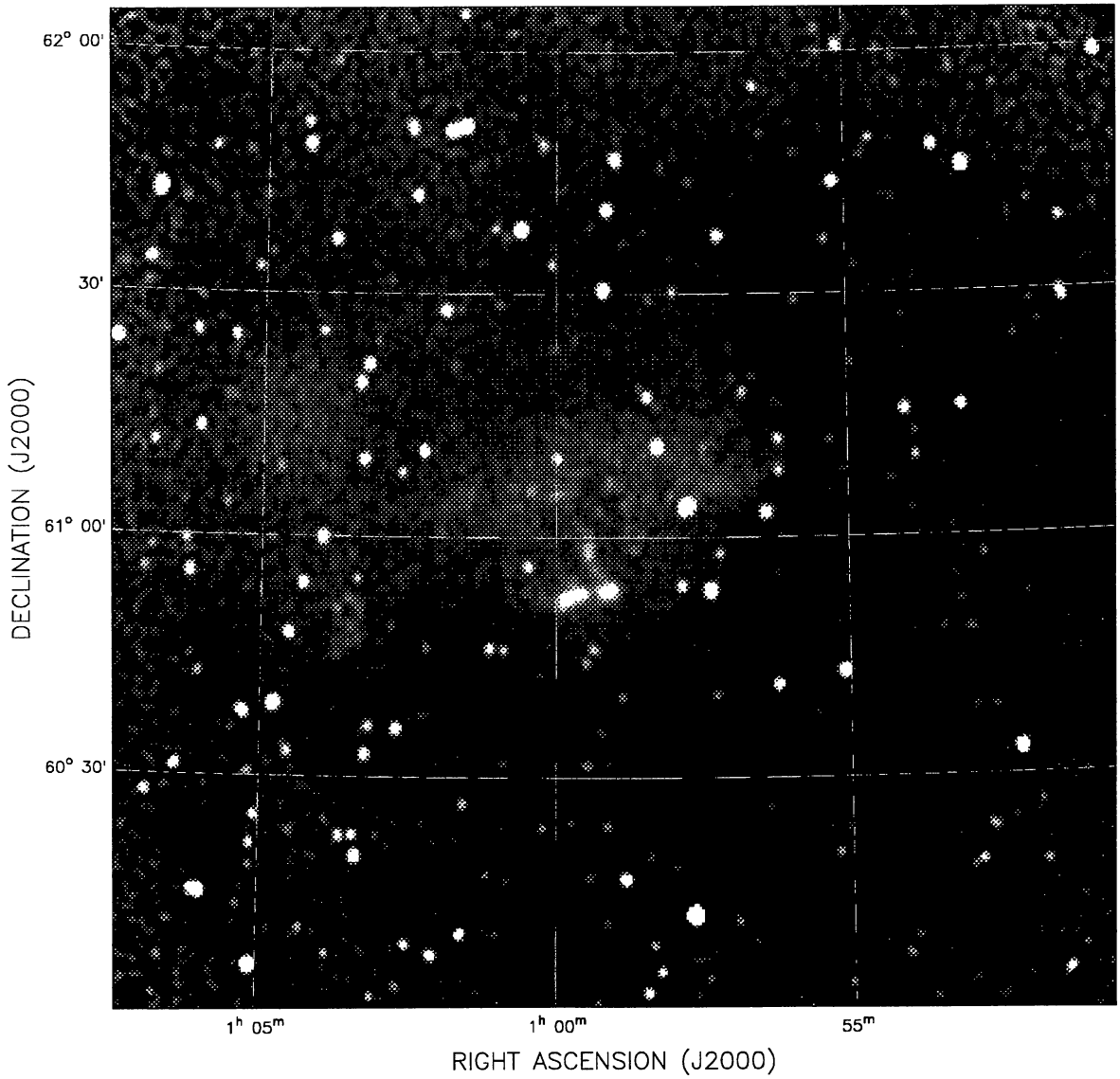

Figure 6. DRAO 21-cm continuum map. One-quarter of the entire field of view is shown. Emission is represented by the grey-scale which varies continuously from 1.0 K (black) to 2.1 K (white).

Table 2. Radio continuum flux densities, S_λ (mJy), and number of ionizing photons, N_L (s^{-1}).

Source	S_{21cm}	S_{74cm}	N_L[1] (10^{44})
IC 63	130±3	130±10	5.9±0.8
IC 59	--	64±3	2.9±0.5
Tip Source	270±20	108±2	--

Notes:
[1]N_L is the number of ionizing photons required to maintain the radio emission.

emission from IC 63 is on the outside of the H I emission, i.e. on the periphery of IC 63, closer to the exciting star.

H I emission from the northern part of IC 59 exhibits small regions or clumps of greater strength, and suffers from confusion with strong emission in the galactic plane. For this work, emission as far north as 61°20′ will be considered to belong to IC 59. H I emission in the southern part of the cloud matches the optical and infrared emission remarkably well (Figs 2 and 5) and the detected cometary shape insures that all three components are associated with each other.

4.3.2 *CO line emission*

The $J=1$–0 CO emission in IC 63 is centrally peaked at the position of peak intensity in the $J=2$–1 and $J=3$–2 maps of Jensen et al. (1994) [$\alpha(1950)=00^h55^m58^s.0$, $\delta(1950)=60°37'07''$] and barely resolved by the FCRAO 45 arcsec beam. The $J=1$–0 peak temperature $T_A^*=4$ K. There is a weak tail of fainter emission which is coincident with the tail of the bright rim of IC 63. In addition to this, a well-confined cloud of emission was detected at the position of IRAS 00556 + 6048 (see Section 4.4).

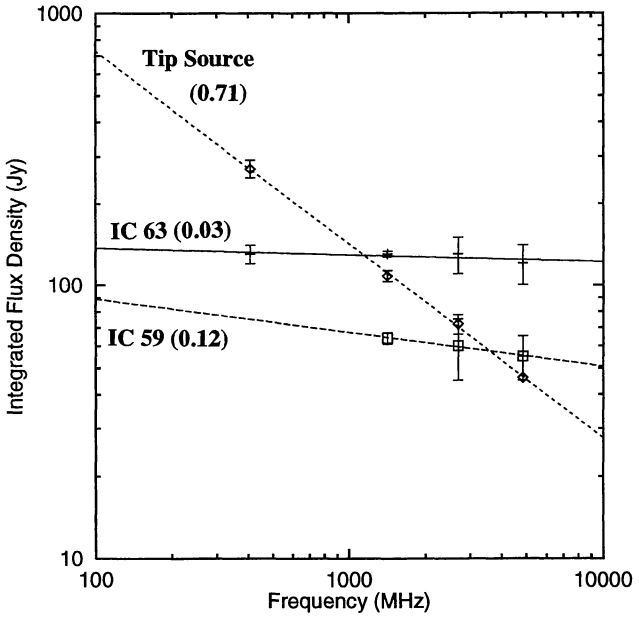

Figure 7. Radio continuum spectra for IC 63, IC 59 and the Tip Source. Numbers in brackets are spectral indices of the emission. The emission from IC 63 and IC 59 is thermal, while that of the Tip Source is non-thermal.

We observed two positions in IC 63 in the $J=2-1$ transition of CO with the JCMT (20 arcsec beam) – the position of peak intensity in the maps of Jansen, van Dischoeck & Black (1994), and a position 2.8 arcmin to the north-east [$\alpha(1950)=00^{h}56^{m}19^{s}.3$, $\delta(1950)=60°38'00''$]. At the position of peak intensity our profile has an integrated intensity $\int T_{A}^{*}\,dV=24$ K km s^{-1} in the 30-arcsec beam of the Caltech Submillimetre Observatory (CSO) telescope. The integrated intensity in the profile from our second position, which is beyond the lowest contour (7 K km s^{-1}) of the map of Jensen et al., is 4.3 K km s^{-1}. Strong $J=2$–1 CO emission was detected at the central position of IRAS 00556 + 6048 (Section 4.4), but no emission was detected at the H I velocity at two positions in IC 59 [$\alpha=00^{h}54^{m}39^{s}.5$, $\delta=60°48'48''$; and $\alpha=00^{h}54^{m}56^{s}.7$, $\delta=60°57'36''$] above the rms noise level of 260 mK.

4.4 An unrelated infrared object in the field of observation

An infrared point source (IRAS 00556 + 6048), believed not to be associated with Sh 185, also appears in our field of observation. It is located midway, in the plane of the sky, between IC 63 and IC 59. There is barely perceptible emission from IRAS 00556 + 6048 on the POSS prints (Figs 2

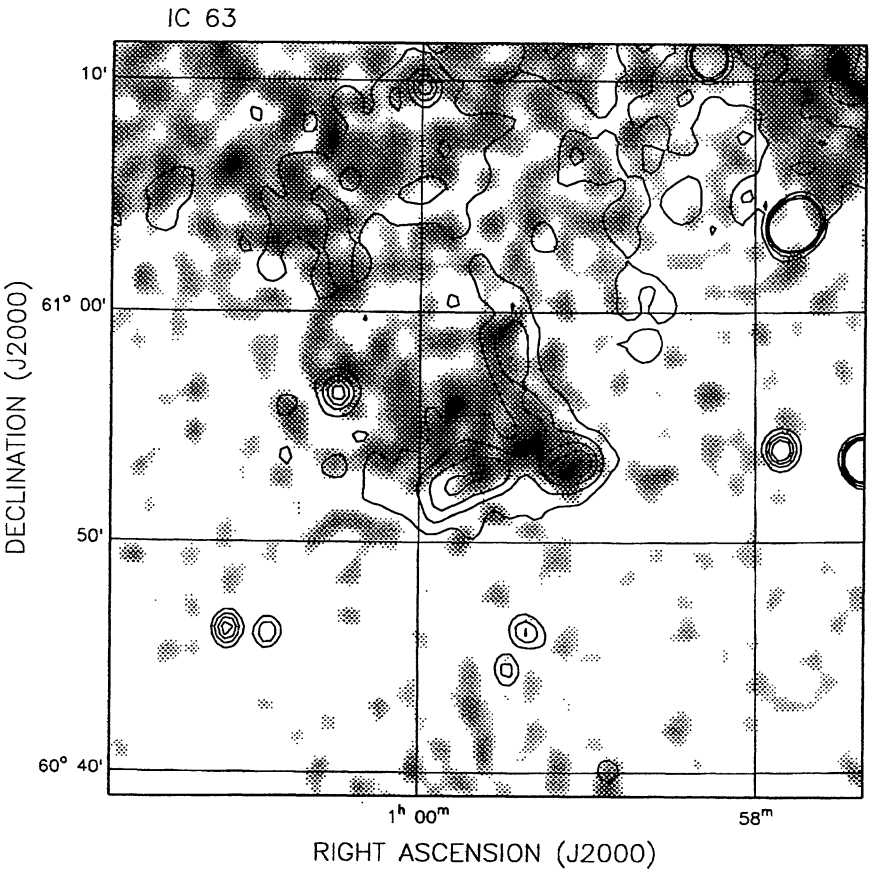

Figure 8. H I column density map for IC 63 [grey-scale: 7×10^{20} atom cm^{-2} (black areas), 5.5×10^{20} atom cm^{-2} (white areas), with a large background component of column density]. Overlying contours of the DRAO 21-cm continuum emission are at 1.5, 1.8, 2.1 and 2.4 K.

and 3). As indicated by a higher dust temperature (Table 1), the spectrum of IRAS 00556 + 6048 appears to peak at a shorter wavelength than those of IC 63 and IC 59.

The distinct far-infrared spectrum of IRAS 00556 + 6048, compared to that of Sh 185, suggests that the source has its own internal source of heating. Both H I and CO ($J=1$–0 and $J=2$–1) emission were detected in association with this source. The $J=1$–0 emission, observed using the 45-m telescope of the FCRAO, has been mapped to delineate an angular size of 3 × 2 arcmin (half-power). The central velocity is -32.5 km s^{-1}. $J=2$–1 emission, at a velocity of -32.7 km s^{-1} ($\int T_A^* dV = 58$ K km s^{-1}), has been observed at only the central position using the 15-m JCMT. Fragmented shell-like structures of H I emission are observed between velocities of -30.7 and -35.7 km s^{-1}. Most of these fragments, located about 5 arcmin away from the infrared peak, with velocity in good agreement with the CO velocity, may be associated with IRAS 00556 + 6048 (Fig. 9). At velocities less than -35.7 km s^{-1} the shell becomes fragmented and only small bits of H I remain. The emission disappears entirely at a velocity of -38.1 km s^{-1}.

The velocities of ≈ -34 km s^{-1} (H I) and ≈ -32 km s^{-1} (CO) translate into a kinematic distance of 1.8 kpc (Brand 1986). At this distance, the mass of atomic gas associated with IRAS 00556 + 6048 is about 4.3 $M_\odot$ with an uncertainty of perhaps 50 per cent due to the imprecise knowledge of what H I is actually associated with the *IRAS* source. The luminosity calculated from the *IRAS* data is 4.7×10^{29} W, which corresponds to the luminosity of a B4 star.

The strong infrared and atomic hydrogen emission together with the non-detection of ionized hydrogen suggest that IRAS 00556 + 6048 could be a dissociating star similar to IRAS 23545 + 6508 discovered by Dewdney et al. (1991). These stars have surroundings of almost entirely dissociated atomic gas, embedded in an environment of molecular gas, in contrast to the earlier stars which ionize the atomic gas and generate substantial H II regions. The influence of B1–B5 stars on surrounding gas can be readily detected from far-IR and H I, emission although the amount of ionization may be insufficient to produce detectable thermal emission. A map of the submillimetre wavelength continuum emission would define a more accurate position of the peak and allow a search for a star of spectral type B4.

We also detected a point source with flux density 65 ± 5 mJy at 74 cm peaking 2 arcmin away from the peak of the infrared source. This continuum source, not detected in any other continuum observations at 21, 11 and 6 cm, is probably not associated with IRAS 00556 + 6048.

4.5 Geometrical assumptions

In order to compare the detected emissions of IC 63 and IC 59 with the stellar properties of γ Cas, the amount of stellar flux incident upon the nebulae must be determined. This requires a knowledge of the entire geometry of the nebulae. Since we do not know the depths of the clouds along the line of sight, we will assume that they are equal to the projected size observed on the POSS prints. Similarily, the distance between the clouds and the exciting star will be assumed to be equal to the observed projected distance (a lower limit to the actual distance). At a distance of 230 pc, this yields 0.13 and 0.17 sr for the solid angles (Ω) subtended by IC 63 and IC 59, respectively, at γ Cas. Taking the tips of the clouds for reference, the star-to-cloud projected distances (d_p) are then 1.3 pc for IC 63 and 1.6 pc for IC 59.

4.6 Comparison with γ Cas

4.6.1 Infrared: energy balance

The far-infrared spectrum of the clouds can be integrated using the formula

$$F_{IR} = (2.5 f_{100} + 4.5 f_{60} + 10.0 f_{25} + 6.5 f_{12}) \times 10^{-14} \text{ (W m}^{-2}\text{)}, \quad (1)$$

where f_λ is the integrated flux density in Jy. This is obtained by approximating the spectrum between the *IRAS* points (including $\lambda = \infty$) with straight lines. At a distance of 230 pc, the luminosities of IC 63 and IC 59 are 1.43 and 1.25 (10^{28}) W respectively. The solid angles of 0.13 and 0.17 sr, subtended at γ Cas by IC 63 and IC 59, represent 1.03 and 1.35 per cent of the total 4π sr subtended at γ Cas. Thus, the maximum luminosity that could be detected from IC 63 and IC 59 if it was all the result of the radiation from γ Cas would be 1.4 and 1.9 (10^{29}) W, respectively. Since the luminosities observed are approximately 10 and 6.6 per cent of these values, the γ Cas luminosity is sufficient to explain the luminosity of the clouds.

4.6.2 Radio continuum: ionization balance

We estimate the masses of ionized gas associated with IC 63 and IC 59 to be 0.08 and 0.07 $M_\odot$, respectively (see Table 3). The number of ionizing photons (N_L) required to maintain the radio continuum emission from IC 63 and IC 59 can be calculated from our flux density measurements using the formula of Rubin (1968). For the electron temperature, we adopt a value of 8000 ± 2000 K, typical of most H II regions. The dependence of N_L on the temperature is weak and the 25 per cent uncertainty on this parameter implies an uncertainty of 10 per cent on N_L. Values for N_L are listed in Table 2. For a solid angle of 0.13 sr, 5.7×10^{44} photon s^{-1} from γ Cas are incident upon IC 63. This is approximately equal to the number of ionizing photons required to maintain the radio continuum emission from the cloud. Therefore, all of the ionizing photons from the star which are impinging upon IC 63 are being used to ionize the gas. This is consistent with the detection of atomic hydrogen in IC 63.

The number of ionizing photons required for IC 59 (2.9×10^{44} photon s^{-1}) is only ~ 50 per cent of the value for IC 63 (Table 2). Since 7.4×10^{44} photon s^{-1} from γ Cas are available to the cloud, 4.5×10^{44} photon s^{-1} are not being used for ionization. The presence of H I in association with IC 59 indicates that the ionized gas component of the cloud is radiation-bounded. This implies that either (1) the missing photons are directly absorbed by dust grains, (2) they are somehow shielded between the star and the cloud, or (3) the geometrical assumptions for IC 59 are incorrect. This problem is discussed further in Section 5.1.

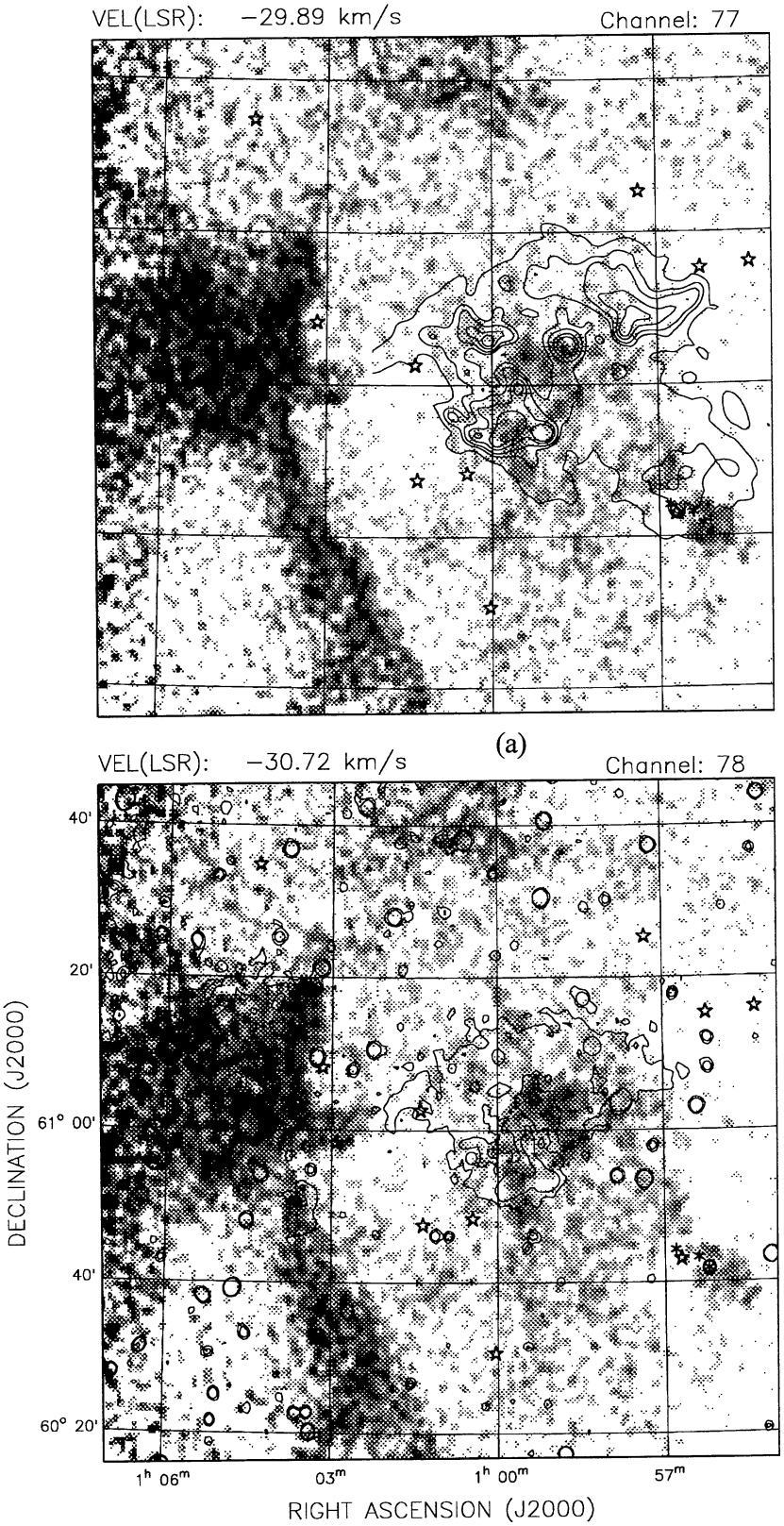

Figure 9. H I emission associated with IRAS 00556 + 6048 [grey-scale: 36 K (black areas), 0 K (white areas)]. Overlying contours of the top and bottom images of (a) and (b), and the five point stars, are the same as for Fig. 4. H I emission was detected over the velocity range −30.72 to −37.31 km s^{-1}, inclusive (channels 78 to 86). (a) Maps for channels 83 and 84 (near the peak of emission).

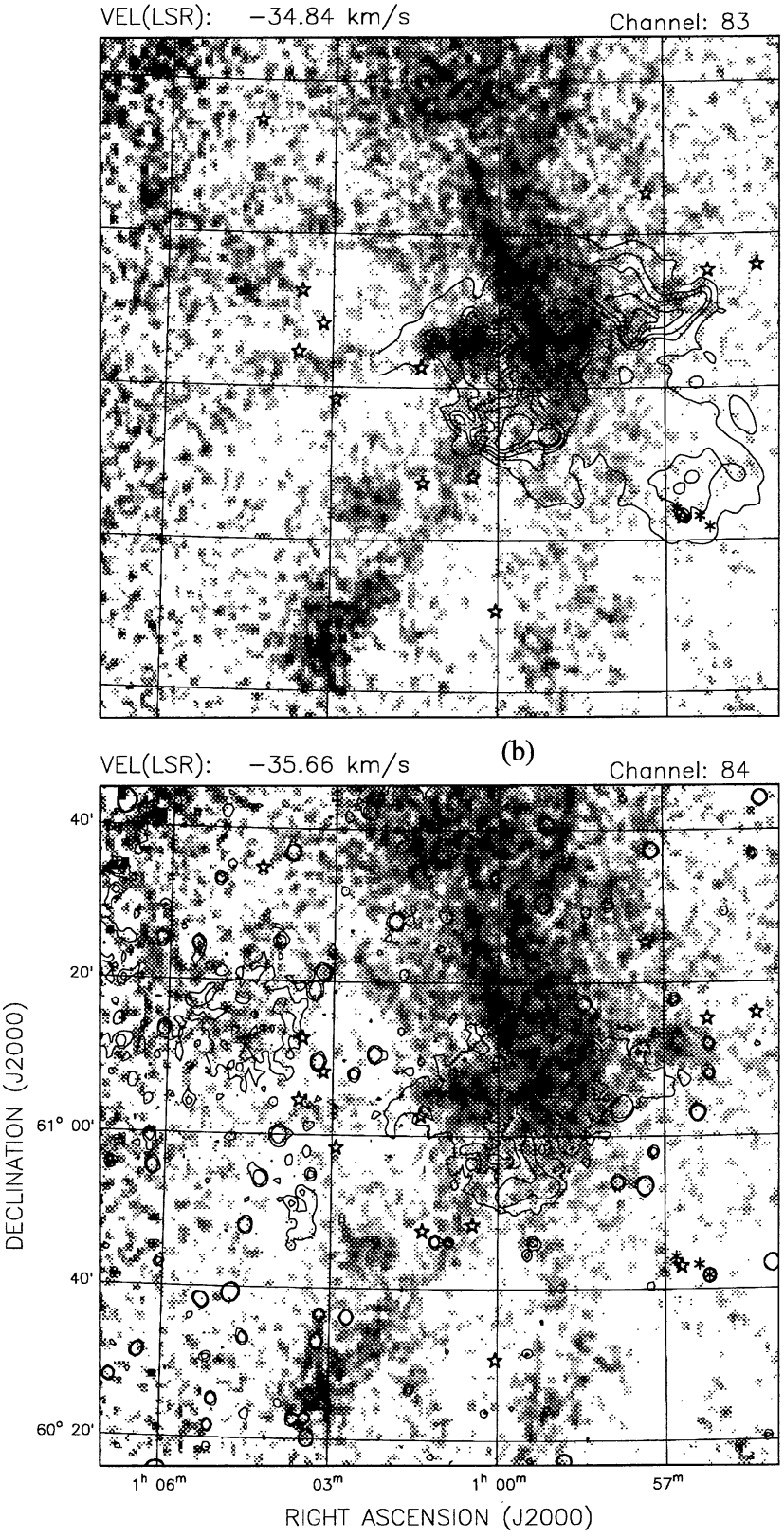

Figure 9 – *continued*

Table 3. H I and H II masses ($M_\odot$).

Source	H I mass	H II mass
IC 63	0.15	0.08
IC 59	0.64	0.07
IRAS 00556+6048	4.3	

4.6.3 *H I line: dissociation balance*

Assuming the 21-cm line emission from IC 63 and IC 59 to be optically thin, we evaluate the masses of atomic gas (Rohlfs 1986) to be 0.15 and 0.64 $M_\odot$, respectively (see Table 3). The mass for IC 59 may be an overestimate since emission in the northern section, which is probably confused with galactic emission, has been included.

The mass of H I can be compared with predictions from the dissociation model of Roger & Dewdney (1992). This dissociation model specifically applies to a radiation-limited case, and simulates the time-development of an H I photodissociation zone in an homogeneous spherically symmetric cloud around a central O–B main-sequence star. Because of the particular geometry of Sh 185, the model was modified to remove any attenuation of starlight resulting from the presence of material between the star and the clouds.

This dissociation model indicates that about 700 yr are required to dissociate the observed mass of atomic gas in IC 63, and 3000 yr to dissociate the molecular gas in IC 59. These times appear to be unrealistically low, being less than the estimated lifetime of γ Cas by 3 orders of magnitudes (see Section 2) and almost certainly indicate that the nebulae are density-bounded and not radiation-bounded, at least in most directions. In the density-bounded case, there is no molecular gas beyond the observed dissociated gas and any photons which are not needed to keep the gas dissociated will simply escape. Comparisons between predictions from the model and the age of the star are then irrelevant. The short dissociation times from the model,a long with the observations of H_2 fluorescent emission and ERE in only IC 63, suggest then that the production of H I from the dissociation of H_2 continues at only a low level in IC 63, and has completely ceased in IC 59. The occurrence in IC 63 of ERE and fluorescence emission of H_2, which trace ongoing photodissociation, is most likely associated with the small molecular cloud detected in CO (see discussion below), and possibly with the bright rims. Here, presumably, the balance between the flux of radiation and gas density is such that an equilibrium is maintained between dissociation and recombination processes. The differences between IC 63 and IC 59 are discussed in the following section.

5 DISCUSSION

Numerous differences between IC 63 and IC 59 noted throughout this paper, and by various authors, are:

(1) colour difference on the POSS prints,
(2) occurrence of bright rims or filaments in one cloud and not in the other,
(3) presence of ERE and UV fluorescence emission in IC 63 only, while H I is detected in both clouds, and
(4) weaker radio continuum luminosity of IC 59 while the IR luminosities of the clouds are similar.

Osterbrock (1957) and Poeckert & van den Bergh (1981) explained the colour difference between the clouds by suggesting that IC 63 is an emission nebula while IC 59 is a pure reflection nebula. If IC 59 is a reflection nebula, this might be the result of the shielding of the γ Cas Lyman continuum radiation by the hypothetical Be disc surrounding the star. The hypotheses of Osterbrock (1957) and Poeckert & van den Bergh (1981) are supported by the weaker radio continuum emission for IC 59, but are not supported by the observations of Witt et al. (1989), which imply that similar excitation conditions prevail in both clouds. According to Witt et al., the redder colour of IC 63 is caused mostly by the presence of ERE.

In this section, we suggest that the differences between IC 63 and IC 59 all result from a difference in the geometry of the clouds. From now on, we will assume that the geometry presented in Section 4.5 holds for IC 63 only.

Osterbrock (1957) and Pottasch (1956), who have studied a number of cometary nebulae, find that the shapes and structures of these clouds depend on the distance from the exciting star. The cometary shapes which evolve in a continuous manner from a flat edge towards a broken shape will exhibit bright rims or filaments on the side toward the exciting star when the cloud is sufficiently close to the star. The bright rims consist of denser regions in the nebula. These regions and the comet-like shape are created by either radiation pressure or shock fronts between media of different density.

Noting that: (1) IC 63 has a more cometary shape than IC 59 [moreover, the cloud does not point exactly towards γ Cas but instead points a few degrees to the east of the star (Figs 1–3)]; (2) IC 59 does not exhibit a bright rim, and (3) the size of IC 59 is larger in the east–west direction than it is in the north–south direction, it is reasonable to presume that the actual distance between IC 59 and γ Cas is larger than the projected distance seen on the prints. If IC 59 is significantly farther than IC 63 from the star, this would explain why the bright rims (or regions of high density) resulting from radiation pressure which are seen in IC 63 are not seen in IC 59. Moreover, the bright rims in IC 63 would be the only place in Sh 185 where molecular material could survive the dissociating radiation from γ Cas because of the higher density in these regions. Consequently, ERE and UV fluorescence emission would occur in IC 63 only.

This hypothesis is supported by various CO observations. Jansen et al. (1994) observed both IC 63 and IC 59 with the CSO telescope and detected CO $J=3$–2 and $J=2$–1 near $V_{LSR}=0$ km s^{-1} only in IC 63, over an area 1×2 arcmin located near the tip of IC 63. At our one position in common with Jensen et al. (see Section 4.3.2), our integrated intensity with a smaller beam is higher. In addition, our map of IC 63 in the ^{12}CO 1–0 line, made with the FCRAO telescope, shows only very weak emission (much weaker than that at $J=2$–1) at the central position. These results are probably the consequence of the molecular material in Sh 185 being localized in small regions of the cloud so that the CO emission suffers from beam dilution.

To estimate the true (or actual) star-to-cloud distance d_{act} and solid angle Ω_{act} for IC 59, we assumed that all ionizing photons from the exciting star which are incident on IC 59 are used to maintain the radio continuum emission, as appears to be the case for IC 63, As in IC 63, this assumption is supported by the detection of H I emission. From equations (A4) and (A5) in the Appendix, we determine $d_{act}=2.65$ pc, and $\Omega_{act}=0.068$ sr if IC 59 is farther from the observer than is γ Cas (i.e. $D_c=232$ pc), or 0.065 sr if it is closer ($D_c=228$ pc). For comparison, the projected distance d_p and corresponding solid angle Ω_p are 1.6 pc and 0.17 sr, respectively.

For a solid angle 0.068 sr, the power from γ Cas incident upon IC 59 is 0.76×10^{29} W. At the distance D_c232 pc, the observed far-infrared integrated flux translates into a total luminosity of 1.27×10^{28} W for IC 59. Therefore, IC 59 absorbs 16.7 per cent of the incident luminosity from γ Cas, which is higher than for IC 63 (10 per cent). The higher absorption through IC 59 is probably a result of its larger depth along the radial direction toward γ Cas. Scaling the projected depth by the factor $d_{act}/d_p=1.66$, we obtain an actual depth of 0.66 pc for IC 59, compared to 0.5 pc for IC 63.

These results indicate that differences between IC 63 and IC 59 can be explained by geometrical differences between the two clouds.

6 CONCLUSION

H I emission was detected in association with IC 63, IC 59, and IRAS 00556+6048, and continuum emission was detected from IC 63 and IC 59. The H I masses are estimated to be 0.15, 0.64, and 4.3 $M_\odot$, respectively. However, the emission toward IC 59 and IRAS 00556+6048 may be partly confused with galactic H I emission. The continuum flux densities for IC 63 and IC 59, and the number of ionizing photons required to maintain the radio emission, are listed in Table 2. The H II masses for IC 63 and IC 59 are estimated to be 0.08 and 0.07 $M_\odot$, respectively. The values for the H I and H II masses are summarized in Table 3.

IRAS 00556+6048 is not believed to be associated with IC 63 or IC 59, and probably is located farther along the line of sight. The associated H I and the lack of radio continuum emission suggest that the exciting star for IRAS 00556+6048 may be another example of a dissociating star as defined by Dewdney et al. (1991).

The continuum emission models suggest that IC 63 is at the same distance as γ Cas, but that IC 59 is farther from γ Cas than IC 63 is. In such a case, the postulated shielding disc surrounding the Be star γ Cas is no longer required to explain the differences between the two nebulae.

Only a small fraction of the incident continuum radiation from γ Cas is re-radiated by IC 63 and IC 59. Most of it passes through the nebulae. Also, the dissociation model of Roger & Dewdney (1992) indicates that the H I masses for IC 63 and IC 59 would be produced by dissociation in the very short times of 700 and 3000 yr. These results imply that the gaseous environment for IC 59 is density-bounded, and that for IC 63 is mostly, but not completely, density-bounded since H_2 fluorescent emission and ERE are still observed there. Thus we conclude that dissociation of H_2 has already ceased in IC 59 but continues at a low level in IC 63. The occurrence in IC 63 of ERE and fluorescence emission of H_2, which trace ongoing photodissociation, is most likely associated with the small molecular cloud detected in CO and the bright rims or filaments in IC 63, where the density is sufficiently high to maintain an equilibrium between dissociation and recombination processes. Further high-resolution line and continuum observations are required to study the bright rims of IC 63. Molecular material may be detected over all of these interesting structures.

ACKNOWLEDGMENTS

We thank Drs Gerald Moriarty-Schieven and Mark Heyer for obtaining CO $J=1$–0 data in the Sh 185 region.

This research has been supported by grants from the Natural Sciences and Engineering Research Council of Canada.

REFERENCES

Assendorp R., Bontekoe Tj. R., de Jonge A. R. W., Kester D. J. M., Roelfsema P. R., Wesselius P. R., 1995, A&AS, 110, 395
Beichman C. A., Neugebauer G., Habing H., Clegg P. E., Chester T. J., 1985, eds, IRAS Explanatory Supplement. Joint IRAS Working Group, U.S. Government Printing Office, Washington DC
Blouin D., 1994, MSc thesis, Univ. British Columbia
Böhm-Vitense E., 1992, Introduction to Stellar Astrophysics, Vol. 3. Cambridge Univ. Press, Cambridge
Bontekoe Tj. R., Koper E., Kester D. J. M., 1994, A&A, 284, 1037
Brand J., 1986, PhD thesis, Univ. Leiden
Condon J. J., Broderick J. J., 1986, AJ, 91, 1051
Condon J. J., Broderick J. J., Seielstad G. A., 1989, AJ, 97, 1064
Cowley A. P., Rogers L., Hutchings J. B., 1976, PASP, 88, 911
Dewdney P. E., Roger R. S., Purton C. R., McCutcheon W. H., 1991, ApJ, 322, 412
Duley W. W., Williams D. A., 1980, ApJ, 242, L179
Fabregat J., Reglero V., 1990, MNRAS, 247, 407
Garrison R. F., Beattie B., 1996, Observer's Handbook. R. Astron. Soc. Can., Univ. Toronto Press, Toronto, Canada
Jansen D. G., van Dishoeck E. F., Black J. H., 1994, A&A, 282, 605
Jones A. P., Duley W. W., Williams D. A., 1990, QJRAS, 31, 567
Kallas E., Reich W., 1980, A&AS, 42, 227
Kogure T., 1990, Ap&SS, 163, 7
Kurucz R. L., 1979, ApJS, 40, 1
Lesh J. R., 1968, ApJS, 17, 371
Osterbrock D. E., 1957, ApJ, 125, 622
Panagia N., 1973, AJ, 78, 929
Poeckert R., van den Bergh S., 1981, PASP, 93, 703
Pottasch S., 1956, Bull. Astr. Inst. Netherlands, 13, 77
Reich W., Fürst E., Reich P., Reif K., 1990, A&AS, 85, 633
Roger R. S., Dewdney P. E., 1992, ApJ, 385, 536
Rohlfs K., 1986, Tools of Radio Astronomy. Springer-Verlag, Berlin, p. 229
Rubin R. H., 1968, ApJ, 154, 391
Slettebak A., 1982, ApJS, 50, 55
Stecher T. P., Williams D. A., 1967, ApJ, 149, L29
Sternberg A., 1989, ApJ, 347, 863
Vakili F., Granes P., Bonneau D., 1984, PASJ, 36, 231
van den Bergh S., 1966, AJ, 71, 990
van der Werf P. P., Dewdney P. E., Goss W. M., vanden Bout P. A., 1989, A&A, 216, 215

Wannier P. G., Andersson B.-G., Morris M., Lichten S. M., 1991, ApJS, 75, 987
Waters L. B. F. M., van der Veen W. E. C. J., Taylor A. R., Marlborough J. M., Dougherty S. M., 1991, A&A, 244, 120
Williams D. R. W., 1973, A&AS, 8, 505
Witt A. N., Schild R. E., 1988, ApJ, 325, 837
Witt A. N., Stecher T. P., Borosan T. A., Bohlin R. C., 1989, ApJ, 336, L21

APPENDIX

If N_{L*} is the total number of ionizing photons emitted by the star γ Cas, and N_{LC} is the number of ionizing photons required to maintain the radio continuum emission of the cloud IC 59, then

$$N_{L*}\frac{\Omega_{act}}{4\pi}=N_{LC} \tag{A1}$$

where Ω_{act} is the actual or true solid angle subtended by the cloud at γ Cas. Using the formula of Rubin (1968),

$$N_{LC}=k_\nu D_C^2\ (s^{-1}), \tag{A2}$$

where

$$k_\nu=4.76\times10^{42}\nu^{0.1}T^{-0.45}S_\nu$$

Here, ν is the observed frequency (GHz), T_e the electron temperature (K) (see Section 4.6.2), S_ν the detected continuum flux density (Jy), and D_C the distance between the cloud and the observer (pc). If the angular width of IC 59 as seen from γ Cas is θ, then

$$\Omega_{act}\approx\frac{\pi\theta^2}{4}.$$

If the angular width of IC 59 as seen by the observer is ϕ, then we can substitute for θ as follows:

$$\Omega_{act}\approx\frac{\pi\left(\frac{\phi D_C}{d_{act}}\right)^2}{4}. \tag{A3}$$

In equation (A3), the distance between the observer and IC 59, D_C, can be expressed in terms of the distance between the observer and γ Cas, D_*, the projected distance between γ Cas and IC 59, d_p, and d_{act}, to obtain,

$$\Omega_{act}=\frac{\pi\theta^2[D_*\pm(d_{act}^2-d_p^2)^{1/2}]^2}{4d_{act}^2} \tag{A4}$$

Using (A1) and (A2) to substitute for Ω_{act} and D_C in (A3), we obtain

$$d_{act}=\frac{\phi}{4}\sqrt{\frac{N_{L*}}{k_\nu}} \tag{A5}$$

The + sign in (A4) is for LC 59 farther from the observer than the exciting star γ Cas, and the − sign is for IC 59 closer.